EVALUATION OF THE RADIATED SOUND POWER OF LIGHTWEIGHT BUILDING CONSTRUCTIONS BASED ON LASER SCANNING VIBROMETER MEASUREMENTS

Maximilian Neusser[1], Armin Wilfling[2], Franz Dolezal[2] und Herbert Müllner[3]

[1] TU Wien Forschungsbereich für Bauphysik und Schallschutz, 1040 Vienna
(maximilian.neusser@tuwien.ac.at)
[2] Holzforschung Austria, 1030 Vienna
[3] Versuchsanstalt am TGM, 1200 Vienna

Abstract

Different measurement methods of radiation efficiency are investigated. The first method uses an intensity probe and a laser vibrometer. The second method is based on the measurement of the sound pressure level in a diffuse sound field. The third method (Discrete Calculation Method - DCM) applies the Rayleigh integral method to calculate the radiated sound power into the semi-infinite space by measuring surface velocity with a laser scanning Doppler vibrometer. In a second step, a finite-element-model of the investigated lightweight building construction is presented. The results of these simulations are compared to the results of the investigated measurement methods.

Keywords: sound radiation, lightweight building construction, Rayleigh, sound insulation

1   Introduction

Referring to the growing importance of the low frequency range in building acoustics, the research community is focusing on acoustic properties of building elements below 100 Hz. At this frequency, ranges we have to deal with non-diffuse sound pressure fields in sending and receiving rooms of laboratories. Traditional measurement methods for the evaluation of the sound reduction index of building constructions rely on the assumption of diffuse sound pressure fields. So new measurement methods have to be found.

1.1   Target

The investigation's target is to evaluate the measurement methods currently existing to determine sound radiation efficiency of building constructions by excitation of airborne and structure-borne sound fields and to examine these methods regarding congruousness. A comparison of the sound pressure and intensity method to determine the radiated sound power as a basis for calculating the sound radiation efficiency was done in Akustik Center Austria's laboratory using a lightweight construction. This construction was excited by airborne and structure borne sound. As a third method, the Rayleigh integral method to estimate the radiated sound power into the semi-infinite space based on measuring the surface velocity with a laser scanning Doppler Vibrometer is investigated, and the results are compared to the conventional methods. Besides the findings gathered by this, validation of a prognosis method of the sound radiation efficiency by modelling the lightweight construction in a Finite Elements Environment is a target of this investigation.

Table 1 – Measurement Method Overview

Method Name	Intensity Method	Sound Pressure Method	Discrete Calculation Method (DCM)
Excitation	Shaker	Loudspeaker	Shaker
Sound Power Measurement	Intensity Probe	-	Rayleigh Model
Sound Pressure Measurement	-	Microphone	Rayleigh Model
Surface Velocity distribution	Laser Vibrometer	Laser Vibrometer	Laser Vibrometer
Construction Mounting	Suspended	Putty	Suspended

2   Measurement setup and construction type

Because of the different measurement methods, the lightweight construction was built into different testing benches under various constraints. The construction consists of two 12.5mm gypsum fiberboards and 100x60x1,250mm wooden studs which were screwed together. The distance between the structural axes is 66cm. Choosing gypsum fiberboards allows for the modelling of one as an isotropic material, thus promising an easy numeric handling than a classic gypsum plasterboard.
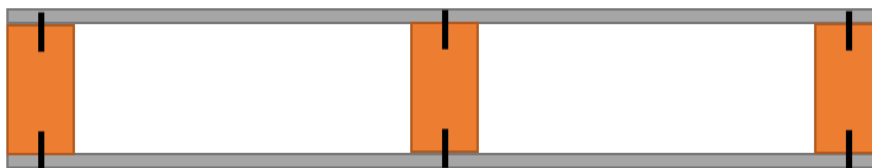
Figure 1 – Schematic representation of the investigated construction type (12.5mm gypsum fiberboard, 100x60mm wooden stud, 12.5mm gypsum fiberboard)

2.1   Stetten

Figure 2 shows the measurement setup for determination of the sound radiation efficiency by using an intensity probe and a laser vibrometer. Here, the construction is hinged on a frame decoupled to prevent the induction of vibratons, and to guarantee a clear modelling of the constraints in the Finite Elements Environment. The Shaker is mounted on a tripod and is coupled to the test specimen via a Stinger and a power sensor.

Figure 2 –Suspended measurement setup.

2.2 TGM

The second measuring arrangement represents a diffuse-diffuse room situation as it is used in classic building acoustics measurements, e.g. the determination of a window's airborne sound insulation. The sound pressure level in the source and the receiving room was determined using microphones and called on to determine the sound power radiated by the wall construction. The lightweight construction was excited with a speaker system using a white noise signal. The velocity distribution on the surface was determined via laser vibrometry in a grid with a point spacing of approx. 10cm.

Figure 3 – Construction mounted by putty into the window measurement frame and reference accelerometer position for the laser vibrometry measurements

Figure 4 shows the speaker system used and installation of the wall construction in the source room's side. The construction was mounted with wood wedges in the testing aperture, the joint coming into being was filled with putty. Then, the wooden wedges were removed to guarantee as free a vibration of the edges as possible.

Figure 4 – Loudspeaker for airborne excitation and backside of the construction mounted by putty into the window measurement frame

3   Numerical modelling

3.1   Material modelling

The formulation of the partial differential equation to determine the material domains' shifts and tensions is implemented in the FEM-environment according to equation 1. Modelling the gypsum fiberboard and the wooden stud is based on the assumption that materials behave linear-elastically. For such materials the correlation betwenn stress and strains can be defined by Hooke's law via the elasticity factor C.

$$-\rho\omega^2\overline{u} = \nabla\sigma + F_V \tag{1}$$

$$\sigma = \sigma_0 + C : (\varepsilon - \varepsilon_0) \tag{2}$$

This elasticity tensor contains the pre-determined material data in its components and the loss-factor determined by [10] in its complex parts (see equation 3).

$$C_c = (1 + i\eta) \cdot C \tag{3}$$

3.2   Fluid structure interaction and boundary conditions

The fluid structure coupling is brought into being by exciting the board within the simualtion environment via the pressure distribution in the fluid media. The board's vibrations are transferred through an appropriate source-term based on the acceleration distribution to the surface adjacent to the fluid. The constraints for the FEM-simulation were assumed as vibrating freely corresponding to the hinged measurement situation. Excitation by the Shaker is modelled using point load at the contruction's working point by the Shaker.

$$\bar{n}(-\frac{1}{\rho}(\nabla p - q\,)) = n \cdot \vec{u}_{tt} \qquad (4)$$

$$F = p \cdot \bar{n} \qquad (5)$$

Where n denotes the normal vector of the construction surface, p is the sound pressure in the fluid medium; u_{tt} is the acceleration of the construction surface and F is the force applied on the construction sruface due to the sound presssure in the fluid medium.

3.3 Junction modelling

Literature provides different methods of modelling the bolted connection, whereby most of the time a linear junction modelling in the frequency range in question (model d) is presumed. Only in higher frequency ranges of the sprectrum >500Hz a punctiform modelling is used. None of the models depicted in figure 6 provides all parameters described in [1] for a physically correct depiction of the connection within the simulation environment. Furthermore, it has been shown in [1,4] that different screw geometry, such as screw head diameter dw, screw length l fand thread pitch P have considerable influence on the stiffness to be expected and the construction's vibration behavior.
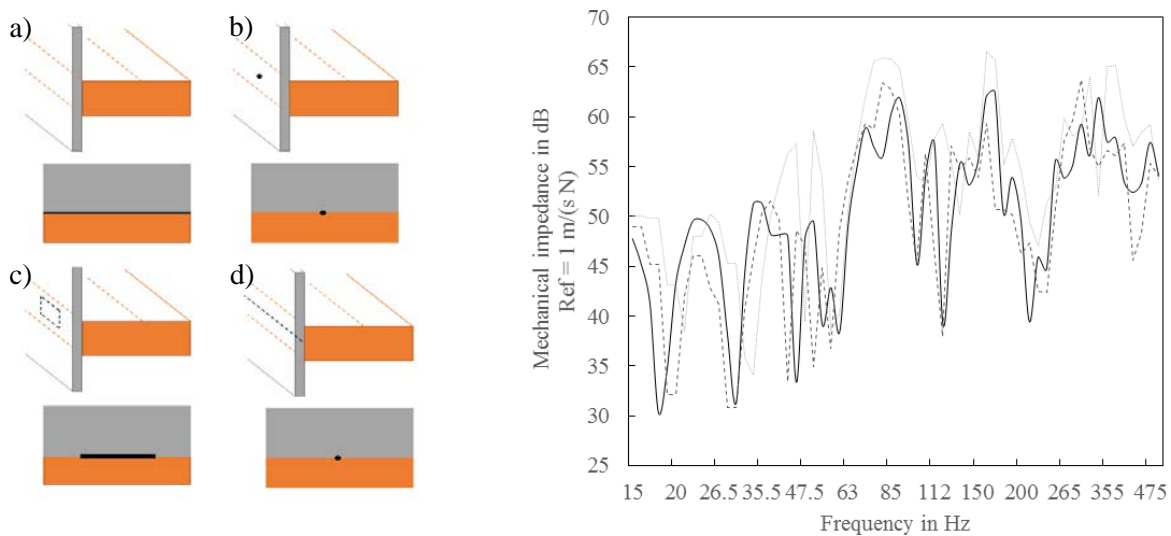
Figure 5 –. Schematic representation of the different junction modelling types [1] (left) and comparison of the simulation (Modell a -··- , Model b ···· , Model c -··-· , Model d - - -) and measurement (solid line) results [1] (right)

To make all these influences depicable, a model following [11] was developed. The model depicts the screw through an equivalently stiff beam, by which an efficient implementation into the FEM-environment is guaranteed. The two shell elements through which the board's clamping to the screw head and the screw tip can be depicted show no significant deformation towards the ceiling and can thus also be efficiently discretised with few elements.
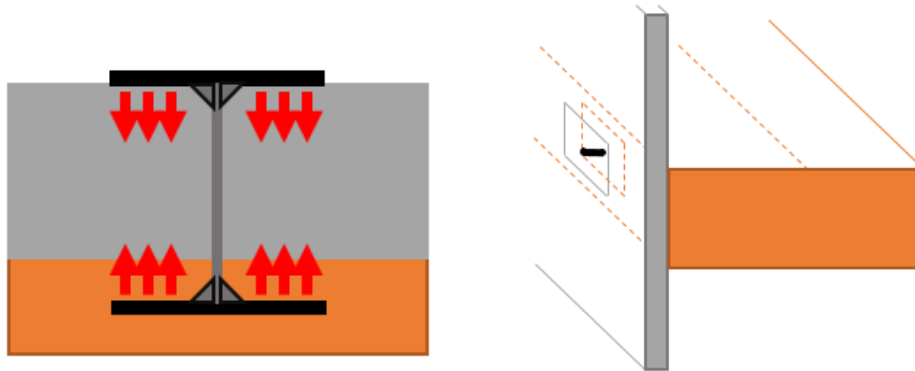
Figure 6 – Schematic representation of the screw model e in the FEM-simulation [1]

The preload force in dependence on the tightening torque (neglecting the friction between screw head and board) is calculated in equation 6 and the shell elements' area are calculated following [11] according to equation 7.

$$F_{pretension} = \frac{M_{torque}}{0.16 \cdot P} \tag{6}$$

$$A_{Shell} = \frac{\pi}{4}\left(d_w + \frac{l_f}{5}\right)^2 \tag{7}$$

4 Material data

The material data of the gypsum fiberboard and the wooden stud was gathered following the method in [3] with the dynamic E-modules set as an absolute value over the entire frequency range of 15-500Hz relevant for this investigation. To depict the attenuation properties, the loss factor was determined by determination of the structure-borne sound reverbaertion period following [2] over the entire frequency range. Table 1 and table 2 show the chosen material parameters for modelling the FEM-environment.

Table 1 – material data wooden stud

E-Module in N/mm²	8950
Poisson's ratio	0.3
Density in kg/m³	400
Isotropic loss factor	0.011 (at 500Hz)

Table 2 – material data gypsum fiberboard

E-Module in N/mm²	4150
Poisson's ratio	0.18
Density in kg/m³	1200
Isotropic loss factor	0.014 (at 500Hz)

5   Measurement and estimation of the sound radiation efficiency

According to table 1 , the sound radiation efficiency of the lightweight construction under structure-borne and airborne excitation was measured using the three described methods. The sound radiation efficiency here is defined as follows:

$$\sigma(\omega) = \frac{\widetilde{W}(\omega)}{\rho_0 c_0 A \left\langle \tilde{v}^2 \right\rangle} \tag{8}$$

W denotes the radiated sound power over the structure surface area *A*, ρ is the density of the air, ω is the angular frequency. The sound power *W* is measured by an intensity probe (intensity method), calcuated based on the sound pressure levels (sound pressure method) in the diffuse sound field and estimated by an Rayleigh integral formulation (DCM). In terms of the DCM and following to [3,5,6,7,12], the sound pressure *p* in distance *d* on Point *r* can be written as

$$\widetilde{p}(\boldsymbol{r},\omega) = \frac{i\omega\rho}{2\pi} \iint_A \widetilde{v}(\boldsymbol{r}_A,\omega) \frac{e^{-ikd}}{d} dS \tag{9}$$

Where *rA* is the position vector on the surface *A,* *d* is the distance between the point of the evaluation and the center of the area *A,* *v* is the velocity in normal direction at the center of the area *A*. The acoustic intensity *I* along the surface *A* of the vibrating panel, in normal direction of the panel, can be obtained as

$$\tilde{I}(\boldsymbol{r}_A,\omega) = \frac{1}{2} Re(\widetilde{p}(\boldsymbol{r}_A,\omega)\tilde{v}(\boldsymbol{r}_A,\omega)) \tag{10}$$

By integrating the intensity over the sound radiating Surface *A,* the total radiated active sound power *W* is calucated.

$$\widetilde{W}(\omega) = \iint_A \tilde{I}(\boldsymbol{r}_A,\omega) dS \tag{11}$$

6   Results and validation

Figure 7 exemplarily shows a comparison between simulation results and measurements in the form of a construction's mechanical impedance following figure 1 with a screw spacing of 27.5cm and a tightening torque of 5Nm for the screws. Various screw spacings and tightening torques were examined. In all cases, satisfying deviations of a maximum of 3dB were achieved.
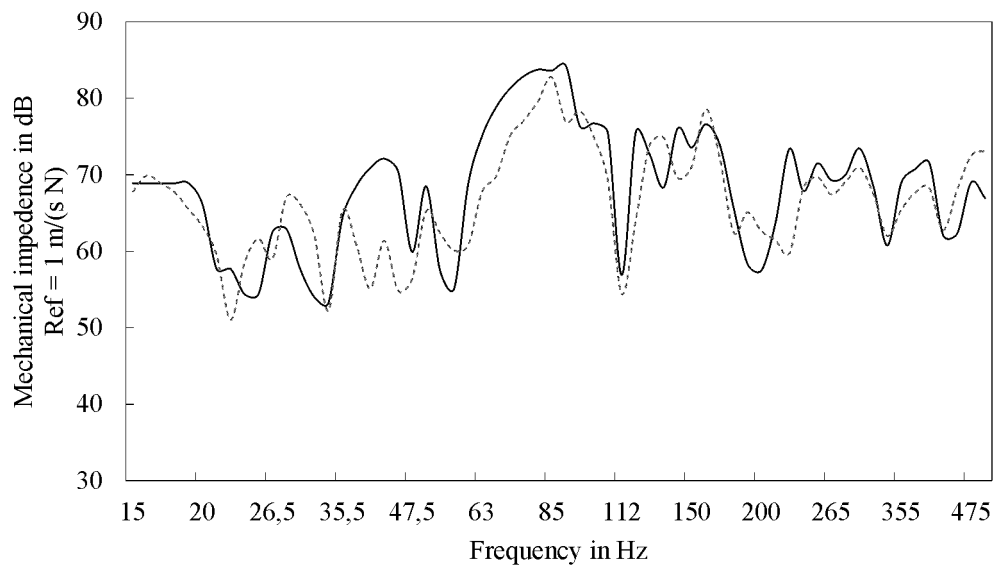
Figure 7 – Comparison between measurement (27.5cm screw spacing, 5 Nm tightening torque– solid line) and simulation result with screw model e (dashed line)

The sound radiation efficiencies determined using the different measurement methods are depicted in figure 8 (left). One can examine differences getting bigger along with the frequency with up to 10dB of the differing sound radiation efficiencies. Figure 8 (right) shows the comparison between the FEM-model's simulation result and the measurement using the DCM-method to determine the construction's sound radiation efficiency.
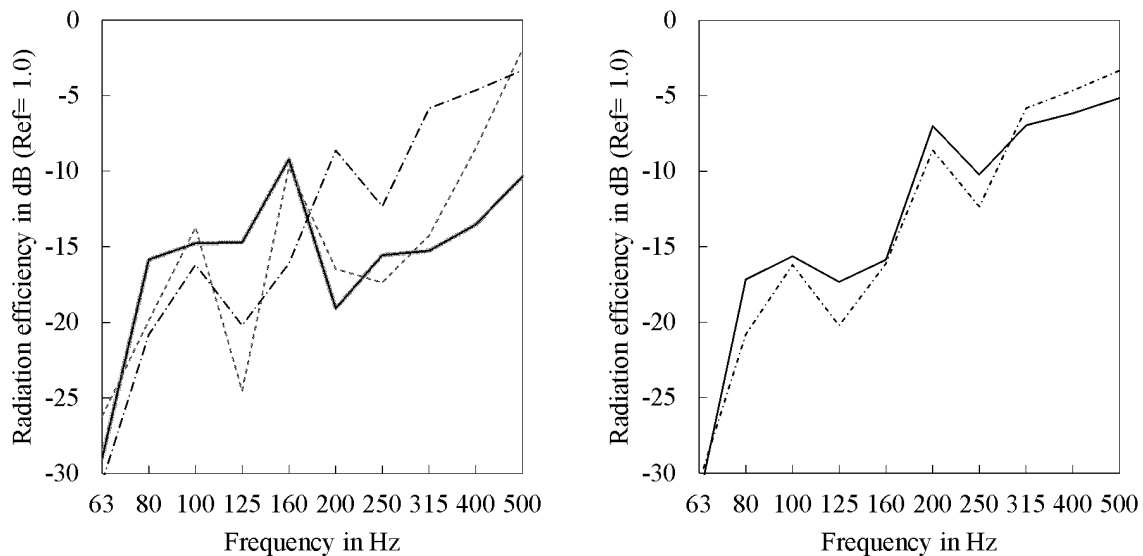
Figure 8 – Comparison of the results of different sound radiation efficiency measurement methods (intensity probe – dashed line; sound pressure method – solid line; DCM – dashed-dotted line) (left) Comparison between DCM result (dashed-dotted line) and the simulated sound radiation efficiency (solid line) (right)

7   Conclusions

The comparison of the sound radiation efficiencies determined using various measurement methods shown in figure 1 (left) shows significant deviations with increasing frequency of up to 10dB. The various constraints of the lightweight-construction's wall-building elements mounting in the various construction situations are a significant influence. The board's edge is mounted freely in the case of the hinged construction, in the window test rig it is constrained by the putty. The boards' edges behavior plays a significant role in the frequency range examined. Although in [10] it was shown that under consistent constraints the measurement methods presented lead to acceptable divergences in results. The comparison between the FEM-model's simulation result and the sound radiation efficiency's measurement using the DCM-method exhibits a lower deviation which is indicative of a good correlation of the mechanical impedance in figure 8 (right) and the equivalent modelling of the sound radiation efficiency based upon it using the Discrete Calculation Method.

References

[1] M. Neusser, A. Wilfling, F. Dolezal, H. Müllner: Modellierung der Schallübertragung einer Gipsfaserständerkonstruktion innerhalb einer Finite Element Umgebung und Validierung durch Laservibrometrie, DAGA, Aachen, 2016

[2] OENORM EN ISO 10848-1:2006-08-01 Akustik - Messung der Flankenübertragung von Luftschall und Trittschall zwischen benachbarten Räumen in Prüfständen - Teil 1

9

[3] ISO/PAS 16940, Glass in building - Glazing and airborne sound insulation - Measurement of the mechanical impedance of laminated glass, 2008.

[4] N. Hashimoto: Measurement of sound radiation efciency by the discrete calculation method. Applied Acoustics 62 (2001) 429-446.

[5] N. B. Roozen, L. Labelle, M. Rychtáriková, C. Glorieux: Determining radiated sound power of building structures by means of Laser Doppler Vibrometry. Journal of Sound and Vibration 346 (2015) 81–99.

[6] H. Muellner, I. Plotizin: Inuence on the airborne sound insulation properties of gypsum plasterboard walls due to minor construction details and workmanship), Proceedings DAGA Bochum 2002

[7] N.B. Roozen, H. Muellner, L. Labelle, M. Rychtarikova, C. Glorieux, Influence of panel fastening on the acoustic performance of light-weight building elements: study by sound transmission and laser scanning vibrometry, Journal of Sound and Vibration, 2015

[8] F.J. Fahy, Sound and Structural Vibration: Radiation, Transmission and Response. Academic Press, London, 1985.

[9] J.S. Lamancusa, Numerical optimization techniques for structuralacoustic design of rectangular panels, Computers & Structures, Volume 48, Issue 4, 17 August 1993, Pages 661-675.

[10] V. Hongisto: Sound insulation of double panels-comparison of existing prediction models. Acta Acustica united with Acustica 92 (2006) 61–78

[11] Hans-Martin Tröbs, Stefan Schoenwald, Armin Zemp: Comparison of different measurement methods of radiation efficiency of lightweight structures, Forum Austicum, Krakau, 2014

[11] Yamamoto A., Theory and Design of Bolt Joints, (1977), pp. 30-69, Yokendo

[12] Rayleigh JWS. The theory of sound. Dover Books. p. 162±9.